ISSN: 2447-3359

REVISTA DE GEOCIÊNCIAS DO NORDESTE

Northeast Geosciences Journal

v. 10, nº 1 (2024)

https://doi.org/10.21680/2447-3359.2024v10n1ID33713

Comparison between geographic object-based and per-pixel approaches for supervised classification of MSI / Sentinel-2 images

Comparação entre abordagens orientada a objetos geográficos e pixel a pixel para classificação supervisionada de imagens MSI / Sentinel-2

Danrlei De Conto[1]; Nilzo Ivo Ladwig[2]; Juliana Debiasi Menegasso[3]; Thaise Sutil[4]

[1] Geoprocsul Engenharia e Geoprocessamento, Criciúma/SC, Brasil. Email: danrleideconto@hotmail.com
ORCID: https://orcid.org/0000-0002-1256-4263

[2] Universidade Federal de Santa Catarina, Programa de Pós Graduação em Geografia, Florianópolis/SC, Brasil. Email: ladwignilzo11@gmail.com
ORCID: https://orcid.org/0000-0003-3031-0192

[3.] Universidade do Extremo Sul Catarinense - UNESC, Criciúma/SC, Brasil. Email: julianaorleans@gmail.com
ORCID: https://orcid.org/0000-0002-2442-6028

[4.] Universidade do Extremo Sul Catarinense - UNESC, Criciúma/SC, Brasil. Email: thaise.sutil@gmail.com
ORCID: https://orcid.org/0000-0001-5766-4260

Abstract: Conventional per-pixel orbital image classification techniques focus only on the spectral features of the image. On the other hand, Geographic Object-Based Image Analysis (GEOBIA) classifiers go further, considering not only spectral features but also characteristics such as shape, size, texture, and spatial distribution. In this context, this study aimed to compare the GEOBIA and per-pixel methods for the supervised classification of land use and cover using high-resolution images. The research was conducted in an area of 72 km² of scene 22JFP captured by the Sentinel-2 satellite. In the GEOBIA method, the steps included image segmentation, feature extraction, and supervised classification using the C4.5 algorithm. In turn, the maximum likelihood algorithm (MAXVER) was employed in the per-pixel approach. The results indicate that the classification using GEOBIA demonstrated higher agreement indices (e.g., Overall Accuracy, Kappa, and Conditional Kappa) than the per-pixel classification. Moreover, the GEOBIA approach achieved higher producer accuracy for classes such as water bodies, mineral waste, bare soil, and shade. In assessing user accuracy, the GEOBIA methodology also showed superior results for urbanized areas, shade, and ground vegetation.

Keywords: Remote Sensing; Land Use; Overall Accuracy.

Resumo: As técnicas convencionais de classificação de imagens orbitais por pixel concentram-se apenas nos atributos espectrais da imagem. Por outro lado, os classificadores baseados em objetos geográficos (GEOBIA) vão além, considerando não apenas os atributos espectrais, mas também características como forma, tamanho, textura e distribuição espacial. Nesse contexto, este estudo tem como objetivo comparar os métodos GEOBIA e Pixel a Pixel para a classificação supervisionada de uso e cobertura da Terra utilizando imagens de alta resolução. A pesquisa foi conduzida em uma área de 72 km² da cena 22JFP capturada pelo satélite Sentinel-2. No método GEOBIA, as etapas incluíram segmentação de imagens, extração de atributos e classificação supervisionada utilizando o algoritmo C4.5. Enquanto isso, na abordagem por pixel, foi empregado o algoritmo de máxima verossimilhança (MAXVER). Os resultados indicam que a classificação por GEOBIA demonstrou índices de concordância (como Exatidão Global, Kappa e Kappa condicional) superiores em comparação com a classificação Pixel a Pixel. Além disso, a abordagem GEOBIA alcançou maior precisão do produtor para classes como massa de água, rejeito mineral, solo exposto e sombra. Na avaliação da precisão do usuário, a metodologia GEOBIA também mostrou resultados superiores para áreas urbanizadas, sombras e vegetação rasteira.

Palavras-chave: Sensoriamento Remoto; Uso da Terra; Exatidão Global.

Received: 25/08/2023; Accepted: 10/04/2024; Published: 24/05/2024.

1. Introduction

There is a significant demand for thematic maps produced through image classification, so performing a comparative analysis between classification methods becomes important in several studies on natural resource management (PINHO et al., 2005; GAO, 2008; BHASKARAN et al., 2010; JEBUR et al., 2013; TEHRANY et al., 2013; COHENCA; CARVALHO, 2015; CHAOFAN et al., 2016; PRUDENTE et al., 2017).

The acquisition of spatial data has become relatively more straightforward with the help of remote sensing technology, which has gained wide acceptance as a reliable source of information (BHASKARAN et al., 2010). Remote sensing orbital data represent a reliable tool for mapping land use and cover dynamics on a large scale at different resolutions (PRUDENTE et al., 2017).

According to Meneses and Sano (2014), image classification methods may be divided according to some criteria, such as parametric or non-parametric, spectral or spatial, and supervised or unsupervised. They are further grouped into classifiers per pixel or object (regions).

Most classifiers perform per-pixel classification while considering only spectral properties of the pixels and using distance or probability measurements to find homogeneous regions belonging to specific classes (MENESES; SANO, 2014). In turn, per-region classifiers also consider textural features, rendering the classification process more similar to the analysis performed by human interpreters, thus resulting in higher accuracy coefficients (BRITES et al., 2014).

From 1980 to 1990, much of the analysis of satellite images was based on statistical algorithms per pixel; since then, one of the most used algorithms for classification based on pixels has been the maximum likelihood (MAXVER) (PRUDENTE et al., 2017). However, over the years, the spectral, spatial, and temporal resolutions of the images have evolved, facilitating accessibility to orbital images with higher resolutions. In this sense, it was necessary to seek new methodologies and techniques that went beyond the per-pixel analysis. One approach that emerged in this process was Geographic Object-Based Image Analysis, known as GEOBIA or OBIA (MORAES, 2018).

In recent years, image classification using the GEOBIA method has received considerable attention for interpreting remote sensing images. GEOBIA resembles the human eye-brain combination, as it uses for the analysis features such as size, texture, shape, and occurrence of the objects in addition to spectral information (ADDINK et al., 2012).

In addition to the various approaches that emerged, it is worth mentioning that new satellite series, such as the Sentinel, have been launched in recent years and provide free images with distinct characteristics. The Sentinel-2 mission aims to monitor variability in Earth's surface conditions through its wide imaging range and high revisit capability. The Sentinel-2 project aims to systematically acquire high-resolution multispectral images with high revisit frequency, to continue the multispectral image series of satellite series such as SPOT and LANDSAT, and to provide observation data for the next generation of operational products, such as land cover maps, change maps, and geophysical variables (ESA, 2014).

Thus, this study aimed to compare the GEOBIA and per-pixel approaches for the supervised classification of land use and cover with high-resolution images.

2. Methodology

2.1 Location and characterization of the study area

The study area is located in the southern region of the state of Santa Catarina, Brazil, covering part of the municipalities of Criciúma and Forquilhinha (Figure 1). The area is bounded by latitudes 28°39'55.03" and 28°44'50.85" South and longitudes 49°26'40.20" and 49°21'41.01" West and extends 7200 hectares. The choice of area was based on the multiplicity of identified land use and cover classes.

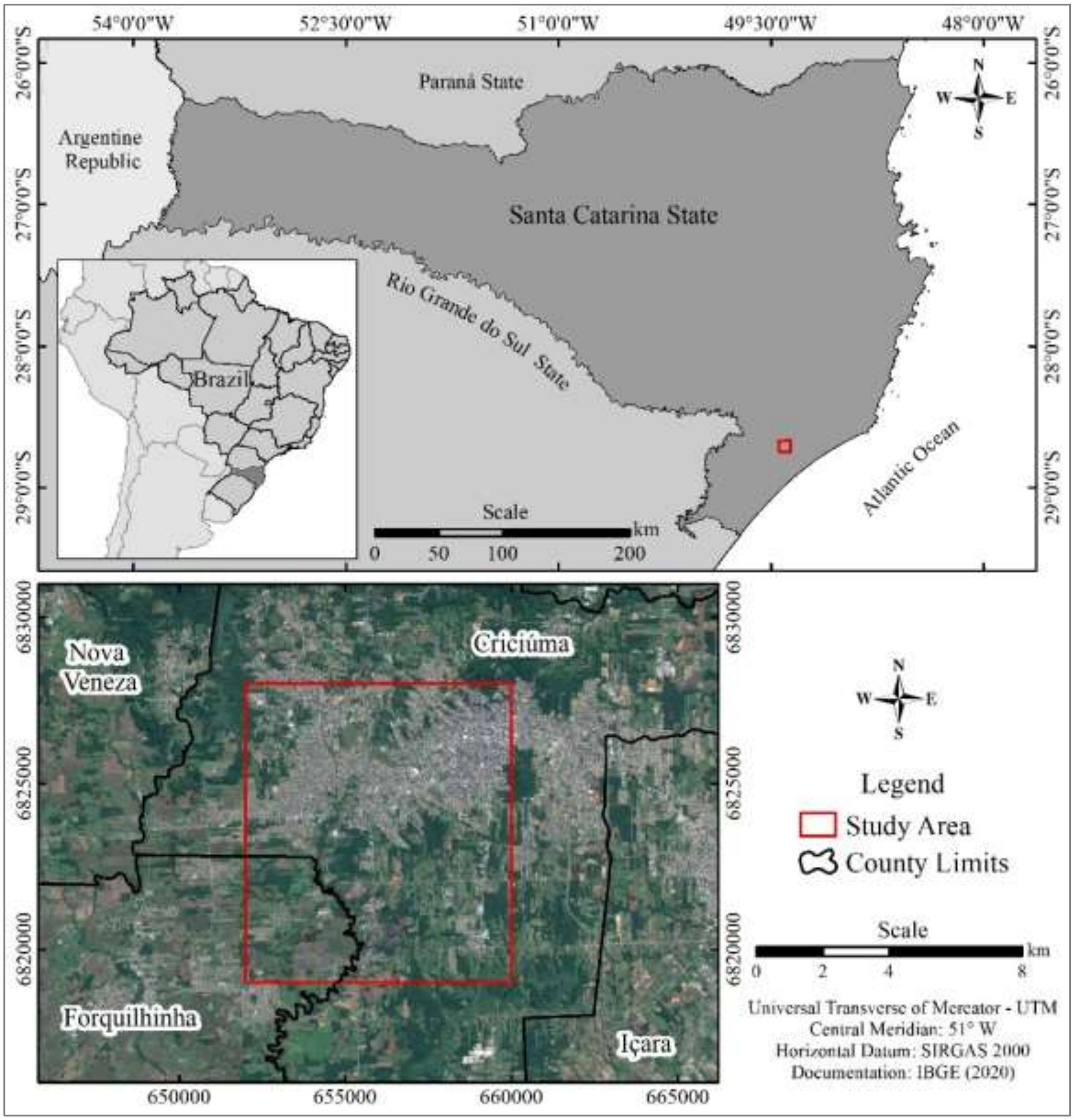

Figure 1 – Location of the study area
Source: Authors (2019).

The methodology adopted in this study followed the flowchart presented in Figure 2. The data selection, image preprocessing, and thematic accuracy analysis processes were the same for the object-based and per-pixel methods used to classify land use and cover in the comparative analysis.

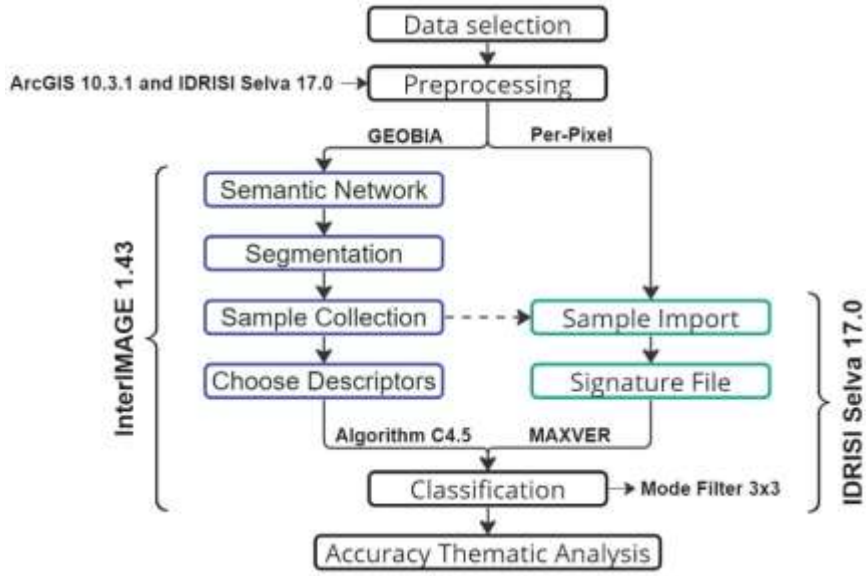

Figure 2 – Study flowchart
Source: Authors (2019).

2.2 Materials used

Ten bands of satellite Sentinel-2B, scene 22JFP, captured by the MSI sensor with spatial resolutions of 10 m and 20 m, were used to carry out the study. Details on the resolution parameters of the images used may be found in Table 1. The images from April 30, 2019, do not show cloud cover and were acquired free of charge on the United States Geological Survey (USGS) Earth Explorer website.

Table 1 – Technical specifications of the MSI sensor bands used

Band No.	Band	Central wavelength (nm)	Bandwidth (nm)	Spatial resolution (m)	Radiometric resolution
2	Blue	492.1	66	10	12 bits
3	Green	559.0	36	10	
4	Red	664.9	31	10	
5	Red Edge 1	703.8	16	20	
6	Red Edge 2	739.1	15	20	
7	Red Edge 3	779.7	20	20	
8	NIR	832.9	106	10	
8a	Red Edge 4	864.0	22	20	
11	SWIR 1	1610.4	94	20	
12	SWIR 2	2185.7	185	20	

Source: Adapted from ESA (2014).

Software was required to execute the preprocessing, processing, and post-processing steps. ArcGIS version 10.3.1 was used to delimit the study area, crop and compose images, and in the evaluation procedures of the thematic accuracy and thematic cartography. InterIMAGE version 1.43 was used to perform the object-based classification steps. In turn, IDRISI Selva version 17.0 was used to improve the contrast of the images and perform the per-pixel classification. The ArcGIS and IDRISI Selva versions used were licensed to the University of the Extreme South of Santa Catarina (UNESC), while InterIMAGE is a free open-source platform.

To enhance the analysis of remote sensing images, preprocessing operations were performed, such as converting the JPEG2000 format to GeoTIFF, cropping the study area, standardizing the spatial resolution, resampling the bands with a spatial resolution of 10 m to 20 m, improving contrast, and composing the ten bands in a single image.

Through visual analysis of the images and prior knowledge of the area of interest, and given the resolution of the images, the classes of land use and cover to be mapped were defined, namely urbanized area, water body, mineral waste, bare soil, shade, arboreal vegetation, and ground vegetation.

2.3 Geographic Object-Based Image Analysis Approach

A new project was created on the InterIMAGE platform, with the composition of the ten bands used in this study as a standard image. Although it is possible to specify in the processing which band or bands will be used, two layers were created for visual interpretation: a composition of the bands R4/G3/B2 (natural color) and a composition of the bands R8/G4/B3 (false color). This numbering does not match that of the sensor.

The semantic network is a knowledge model used to interpret an image. However, for classification with the C4.5 algorithm, all classes must be at the same hierarchical level. A semantic network with one node for each land use and cover class. It was established in this network that all classes were at the same hierarchical level (Figure 3).

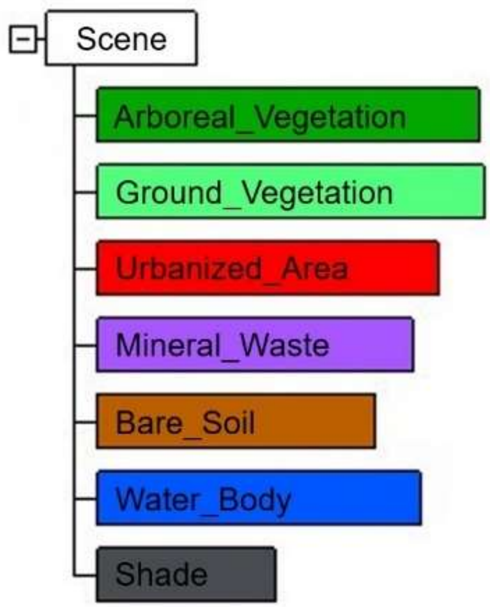

Figure 3 – Semantic network established
Source: Authors (2019).

The segmentation of the image and the collection of training samples were performed using the Samples Editor menu. The segmentation was performed by the TA_Baatz_Segmenter algorithm proposed by Baatz and Schäpe (2000), using weight 1 for all bands, compactness weight 0.8, color weight 0.5, scale parameter 120, reliability 0.2, and Euclidean distance threshold 20 as input parameters.

Sample segments were collected to indicate the characteristics of each class to the classification algorithm. The sampled and the remaining segments were then exported to the shapefile format with spectral and shape descriptors. The descriptors used were mean, entropy, band list, brightness, area, compactness, segment length and width, Normalized Difference Vegetation Index (NDVI), Normalized Difference Bare Soil Index (NDBSI), and Normalized Difference Water Index (NDWI).

The classification was performed by assigning the top-down operator TA_C45_Classifier to the first node of the semantic network, defining the segmentation file containing the samples and the descriptors in the Training Set File and Input Shape File fields.

2.4 Per-Pixel Approach

To avoid the subjectivity of the sample collection, the same sampling areas used with GEOBIA were used in the per-pixel classification. For this, the sample file in shapefile format was imported into IDRISI Selva version 17.0. However, due to database incompatibilities, the signature file could not be created, so each of the sample polygons had to be digitized.

From the sample areas, the signature file was created, and the classification was performed using the MAXVER algorithm with equal probability for all classes of interest. As suggested by Crosta (1992), a mode filter with a 3x3 window was applied to remove isolated pixels.

2.5 Accuracy Analysis

When evaluating the thematic accuracy of classes with small areas, the stratified random distribution is more appropriate. The minimum number of reference points for areas under 400 km² with less than 12 classes should be 50 points per class (CONGALTON, 1988; 1991).

Thus, a mesh with 350 reference points was generated to evaluate the thematic accuracy, with 50 points in each class of land use and cover generated through object-based classification. The mesh was generated using the ArcGIS Create Random Points tool.

By photointerpretation, the reference points were evaluated as to the class of land use and cover and received the code of the corresponding class. Finally, the points were crossed by intersection with the generated maps and the frequency was analyzed using the ArcGIS Spatial Join and Frequency tools.

2.5.1 Confusion Matrix

One of the most used techniques in assessing classification accuracy is the Confusion Matrix, also known as the Error Matrix (CONGALTON, 1991). In this study, the matrix was used as a starting point for a series of descriptive and analytical statistical techniques, as suggested by Suarez and Candeias (2012).

According to Congalton and Green (2009), this matrix is a very effective representation of the accuracy of the generated classification, given that the individual accuracies of each class are described, taking into account the errors of inclusion and omission. An inclusion error occurs when an area is included in a class to which it does not belong, while an omission error occurs when an area is excluded from the class to which it belongs.

The Confusion Matrix is a square matrix of numbers defined in rows and columns that express the number of units of the sample (pixel or object) assigned to a particular category relative to the current category. Typically, the columns represent the reference data and the rows the classification generated (SUAREZ; CANDEIAS, 2012). Thus, a Confusion Matrix was assembled with the generated data, allowing the calculation of accuracy parameters.

2.5.2 Overall, Producer, and User Accuracy

The Overall Accuracy index is a descriptive statistic proposed by Helldén (1980). According to Congalton and Green (2009), it is the sum of the main diagonal of the Confusion Matrix (correctly classified units) divided by the total number of units in the sample.

The probability that a reference sample (pixel or object) will be classified correctly (the measure of the omission error) is known as Producer Accuracy. When the total number of correct samples in a class is divided by the total number of samples classified in the class, one has the measure of the inclusion error, known as User Accuracy (SUAREZ; CANDEIAS, 2012). Hence, based on the Confusion Matrix, the Overall, Producer, and User Accuracies were calculated for the two classification approaches.

2.5.3 Kappa

The Kappa index is a coefficient of agreement for nominal scales that assesses the proportion of agreement. Its importance is justified because it uses all the elements of the Confusion Matrix (COHEN, 1960).

From the Confusion Matrix, it is possible to use analytical statistics techniques such as multivariate discrete techniques, given that they are appropriate since the classification data are discrete, not continuous. The data are also normally distributed (CONGALTON, 1988).

The Kappa index proposed by Cohen (1960) is a multivariate discrete technique that may be expressed by Equation 1, where K is the coefficient of agreement Kappa, $P_O = \frac{\sum_{i=1}^{M} n_{ii}}{N}$ represents the portion of agreeing reference points, $P_{CO} = \frac{\sum_{i=1}^{M} n_{i+} n_{+i}}{N^2}$ represents the portion of points assigned at random, N is the total number of points of the confusion matrix, n is the element of the confusion matrix, n_{ii} are elements of the main diagonal of the confusion matrix, n_{i+} is the sum of the row for a given thematic class, and n_{+i} is the sum of the column for a given thematic class.

$$K = \frac{P_O - P_{CO}}{1 - P_{CO}} \tag{1}$$

In addition to the Kappa index, one may calculate the conditional Kappa, which aims to evaluate the accuracy of each thematic class and is calculated based on the same principle used for the overall assessment of the classification (CONGALTON; GREEN, 2008). It may be expressed by Equation 2:

$$K_C = \frac{N x_{ii} - x_{i+} x_{+i}}{N x_{i+} - x_{i+} x_{+i}} \tag{2}$$

The Z test (CONGALTON; GREEN, 2008) was used, according to Equation 3, to test the statistical significance of the difference between the two calculated Kappa indices (GEOBIA and per-pixel), where K_1 is the Kappa index of the GEOBIA classification, K_2 is the Kappa index of the per-pixel classification, and σ^2 is the variance of the Kappa index.

$$Z = \frac{k_2 - k_1}{\sqrt{\sigma_{k_2}^2 + \sigma_{k_1}^2}} \tag{3}$$

3. Results and Discussion

3.1 Geographic Object-Based Image Analysis Approach

The GEOBIA classification showed the predominance of the urbanized area (34.29%), ground vegetation (33.67%), and arboreal vegetation (22.59%) classes, with the shade and water body classes jointly representing less than 1% of the study area (Table 2 and Figure 4).

Table 2 – Areas using the object-based approach

Use and Cover Classes	Area (ha)	%
Urbanized area	2468.71	34.29
Water body	36.14	0.50
Mineral waste	75.40	1.05
Bare soil	544.31	7.56
Shade	24.74	0.34
Arboreal vegetation	1626.35	22.59
Ground vegetation	2424.35	33.67
Total	7200.00	100.00

Source: Authors (2019).

In Figure 4, one may visually identify, in the northeast quadrant of the study area, the presence of regions of the shade and mineral waste classes in the middle of a large region of the urbanized area class. This shading may be due to the fact that this is a verticalized urban area. On the other hand, the classification of mineral waste areas involves conflicts with partially shaded areas of paving and dark roofs, which presented a spectral response similar to this class.

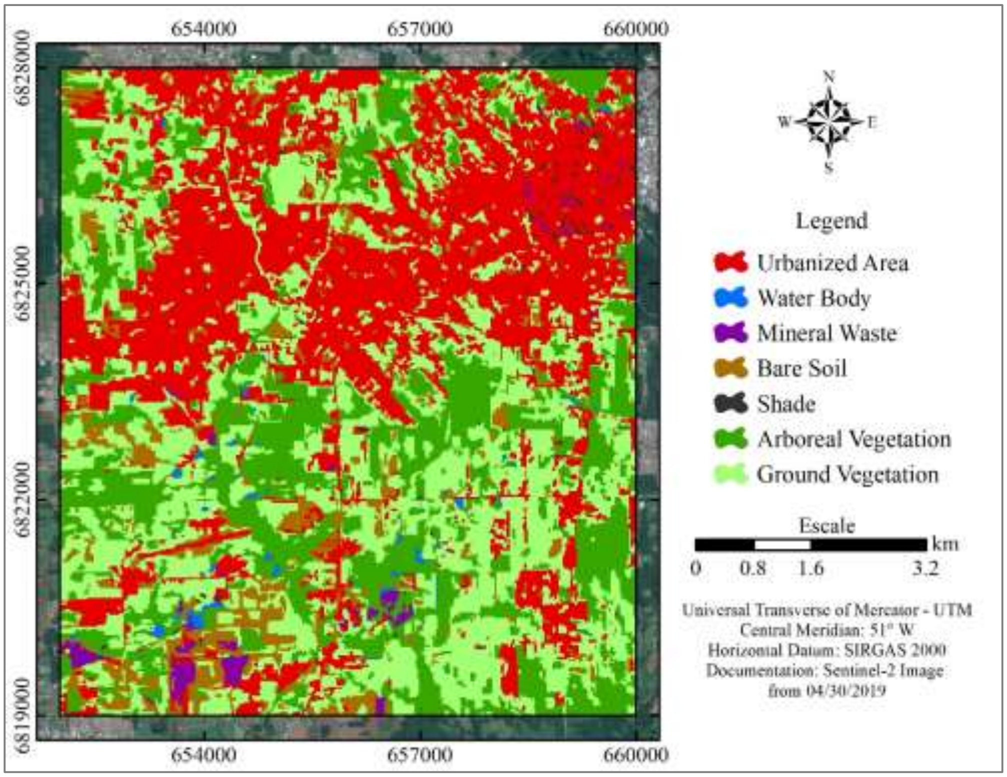

Figure 4 – Land use and cover according to GEOBIA
Source: Authors (2019).

The confusion matrix represents the relationship between the mapped classes and the reference data. Table 3 contains the confusion matrix generated from the thematic mapping according to GEOBIA and the 350 reference points. The main diagonal of the confusion matrix represents the points at which the classification was successful, highlighting the urbanized area class followed by the arboreal and ground vegetation classes. The class that presented the least hits at the reference points was the shade class.

The values outside the main diagonal represent classification errors, with no agreement between reference points and the classification product. The most significant error source in the classification of nine urbanized areas was in the shade class. Expressive errors were also observed between the urbanized area and bare soil classes, the arboreal vegetation and water body classes, and the ground vegetation and bare soil classes.

Table 3 – Confusion matrix for the object-based classification

	Reference Datum								
	Classes	WB	MW	BS	SH	UA	AV	GV	**Total**
Classified Datum	WB	34	0	2	3	4	7	0	**50**
	MW	0	41	1	3	5	0	0	**50**
	BS	0	0	34	1	7	1	7	**50**
	SH	1	5	2	25	9	6	2	**50**
	UA	0	1	2	0	46	0	1	**50**
	AV	0	0	0	0	0	42	8	**50**
	GV	0	0	2	0	1	5	42	**50**
	Total	**35**	**47**	**43**	**32**	**72**	**61**	**60**	**350**

WB – Water body, MW – Mineral waste, BS – Bare soil, SH – Shade, UA – Urbanized area, AV – Arboreal vegetation, and GV – Ground vegetation

Source: Authors (2019).

3.2 Per-Pixel Approach

As observed in the GEOBIA classification, in the per-pixel classification, the urbanized area class was the most expressive, representing 39.93% of the area, followed by the ground vegetation (30.54%) and arboreal vegetation (21.82%) classes. On the other hand, the water body (0.38%) and mineral waste (0.90%) classes were less expressive (Table 4 and Figure 5).

Table 4 – Areas using the per-pixel approach

Use and Cover Classes	Area	
	Hectares	%
Urbanized area	2874.72	39.93
Water body	27.08	0.38
Mineral waste	64.44	0.90
Bare soil	311.64	4.33
Shade	152.56	2.12
Arboreal vegetation	1570.76	21.82
Ground vegetation	2198.80	30.54
Total	**7200.00**	**100.00**

Source: Authors (2019).

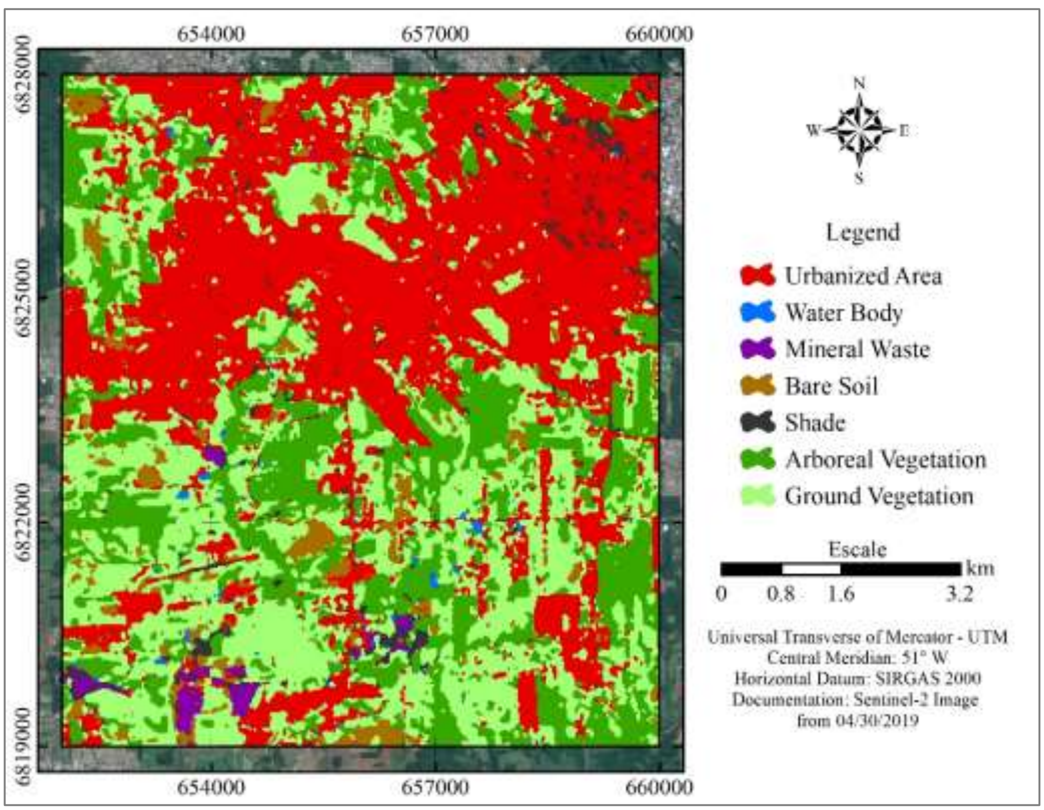

Figure 5 – Land use and cover according to the per-pixel approach
Source: Authors (2019).

The supervised classification performed by the MAXVER algorithm (Figure 5) presented, as in the GEOBIA classification, several areas of the shade class in the most vertical urban portion, in addition to shade class polygons scattered throughout the study area, especially near the mineral waste areas. Unlike the GEOBIA classification, the per-pixel classification did not present conflicts between the mineral waste and urbanized area classes in vertical urban portions.

Regarding accuracy (Table 5), the mineral waste class presented the most classification hits when the reference points were analyzed, followed by the bare soil and arboreal vegetation classes. In turn, the shade class had a poor result, presenting many conflicts with the urbanized area, water body, and mineral waste classes, the latter being classes with low albedo in most bands of the reflected optical spectrum, having little spectral contrast relative to the shade. An expressive conflict also occurred between bare soil and ground vegetation, which may result from the existence of areas with low or sparse vegetation.

Table 5 – Confusion matrix for the per-pixel classification

	Reference Datum								
Classified Datum	Classes	WB	MW	BS	SH	UA	AV	GV	**Total**
	WB	20	1	0	1	0	2	0	**24**
	MW	0	33	0	0	1	1	1	**36**
	BS	1	1	23	1	1	0	0	**27**
	SH	12	11	2	20	12	6	1	**64**
	UA	0	1	4	9	57	1	7	**79**
	AV	0	0	1	1	0	46	6	**54**
	GV	2	0	13	0	1	5	45	**66**
	Total	**35**	**47**	**43**	**32**	**72**	**61**	**60**	**350**

WB – Water body, MW – Mineral waste, BS – Bare soil, SH – Shade, UA – Urbanized area, AV – Arboreal vegetation, and GV – Ground vegetation

Source: Authors (2019).

3.3 Comparison: GEOBIA × Per-Pixel

The quantitative data of areas by the two classification methods are presented in Table 6. In addition to being the largest in both classifications, the urbanized area class was also the one with the most significant difference in area between the methods. Attention is also drawn to the difference in the shade and bare soil classes, given that both exhibit considerable differences proportional to the areas. The arboreal vegetation class had the highest agreement in both methods.

Table 6 – Areas of the land use and cover classes

Use and Cover Classes	GEOBIA		Per-Pixel	
	Area (ha)	%	Area (ha)	%
Urbanized area	2468.71	34.29	2874.72	39.93
Water body	36.14	0.50	27.08	0.38
Mineral waste	75.40	1.05	64.44	0.90
Bare soil	544.31	7.56	311.64	4.33
Shade	24.74	0.34	152.56	2.12
Arboreal vegetation	1626.35	22.59	1570.76	21.82
Ground vegetation	2424.35	33.67	2198.80	30.54
Total	**7200.00**	**100.00**	**7200.00**	**100.00**

Source: Authors (2019).

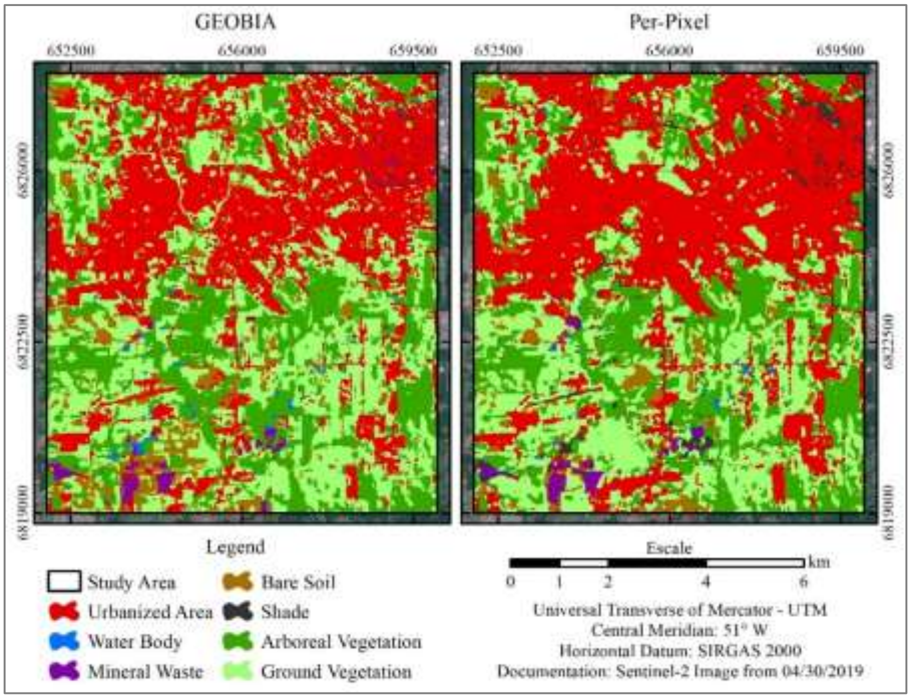

Figure 6 – Land use and cover: GEOBIA and Per-Pixel
Source: Authors (2019).

Visually comparing the generated maps (Figure 6), the GEOBIA classification showed more significant detailing in the geometry of the forms of use and cover, while the per-pixel classification appears more generalistic. In the work carried out using Ikonos images, Pinho et al. (2005) identified that, in general, the results using GEOBIA better preserved the geometry of the targets of interest.

The GEOBIA result shows greater coherence in classifying shaded areas, limiting them to the most vertical urban areas. However, the per-pixel classification is more successful in mapping the mineral waste class, showing no conflicts in urban areas

.

3.3.1 Analysis of thematic accuracy

With the error matrices, the agreement coefficients that indicate the total and individual accuracy of each class were calculated. When evaluated in general, the GEOBIA classification presented 75.43% overall accuracy and a Kappa index of 71.33% (Figure 7). The per-pixel classification also generated good results, albeit lower than the previous ones, with an overall accuracy of 69.71% and a Kappa index of 64.26%.

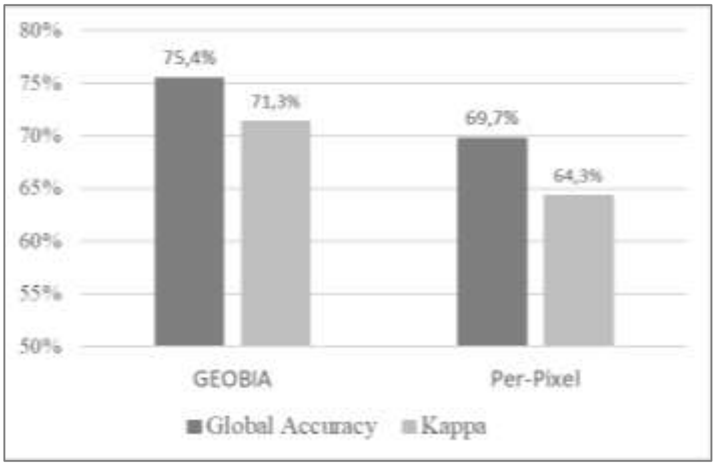

Figure 7 – Coefficients of total agreement
Source: Authors (2019).

It is possible to observe that in both approaches, the Kappa index presented lower agreement values than in the overall accuracy. According to Cohen (1960), this difference may be due to the use of all matrix cells in calculating the Kappa index, thus including the errors of omission and inclusion of classes.

The pattern in the coefficients of total agreement found in this study is similar to those found by Gao (2013), JEBUR et al. (2013), Chaofan et al. (2016), Qiu et al. (2017) and Prudente et al. (2017). On the other hand, Cohenca and Carvalho (2015) obtained coefficients of total agreement for the per-pixel classification higher than those for GEOBIA, which may have occurred due to the spatial resolution (30 m) of the study image.

From the error matrix, it is possible to calculate accuracy measures individually for each thematic class, such as producer and user accuracy (Table 7). In the GEOBIA classification, the water body class presented 97.1% producer accuracy, and the lowest producer accuracy was for the urbanized area class, with 63.9% and 36.1% of omission error. Regarding user accuracy, urbanized areas obtained 92.0%, i.e., only 8% of inclusion error. In turn, the shade class obtained only 50% accuracy.

Table 7 – Accuracy by thematic class of land use and cover

Use and Cover Classes	GEOBIA		Per-Pixel	
	PA (%)	UA (%)	PA (%)	UA (%)
Urbanized area	63.9	92.0	79.2	72.2
Water body	97.1	68.0	57.1	83.3
Mineral waste	87.2	82.0	70.2	91.7
Bare soil	79.1	68.0	53.5	85.2
Shade	78.1	50.0	62.5	31.3
Arboreal vegetation	68.9	84.0	75.4	85.2
Ground vegetation	70.0	84.0	75.0	68.2

PU – Producer Accuracy; UA – User Accuracy

Source: Authors (2019).

Regarding the producer accuracy, the per-pixel classification presented 79.2% in the urbanized area class as the best result, in addition to two classes with less than 60% accuracy: bare soil with 53.5% and water body with 57.1%, values considered regular. In terms of user accuracy, the mineral waste class presented 91.7% accuracy or 8.3% inclusion error. The shade areas, however, were mapped with only 31.3% accuracy, with 68.7% inclusion error.

As with the coefficients of total agreement, in class-by-class accuracy (producer and user), the GEOBIA classification showed accuracy higher than the per-pixel classification.

In addition to the indices already calculated, we also decided to calculate the conditional Kappa (Table 8). In the analysis, it was determined that the classes in both classifications presented differences. The difference was little significant in the arboreal vegetation class, while larger differences were observed in the others. As with other coefficients already calculated, the shade class presented the most considerable difference.

Table 8 – Conditional Kappa of land use and cover

Use and Cover Classes	GEOBIA	Per-Pixel
Urbanized area	64.44	81.48
Water body	79.21	90.37
Mineral waste	63.52	83.11
Bare soil	44.97	24.33
Shade	89.93	64.94
Arboreal vegetation	80.62	82.06
Ground vegetation	80.69	61.60

Source: Authors (2019).

In general, the GEOBIA approach presented higher agreement coefficients than the per-pixel classification. The hypothesis test performed between the Kappa indices showed that, at a level of 5%, there was no significant difference (z = 1.81) in accuracy between the two approaches. Therefore, the GEOBIA classification did not increase accuracy significantly at a 95% confidence interval. It is noteworthy that, for a 90% confidence interval, the difference would be significant according to the normal distribution pattern (CONGALTON; GREEN, 2008).

4. Final considerations

In this work, we compared the GEOBIA and per-pixel approaches to classifying land use and cover in high-resolution images. The results obtained for the agreement coefficients (overall accuracy, Kappa, and conditional Kappa) showed that the GEOBIA classification obtained superior results compared to the per-pixel classification. The hypothesis test showed that, with a 95% confidence interval, there was no significant difference.

The GEOBIA approach presented more considerable producer accuracy than the per-pixel classification for water bodies, mineral waste, bare soil, and shade classes. In analyzing user accuracy, the GEOBIA approach provided superior results for the urbanized area, shade, and ground vegetation. The arboreal vegetation class had similar results in both approaches (difference of 1.2).

In general, the GEOBIA classification statistically demonstrated the method indicated for Sentinel-2 image analysis. However, more theoretical depth is needed to obtain more expressive results, given that no studies were found in the literature comparing the two approaches for these images.

In this sense, it is recommended that future studies be carried out to explore different methodologies for analyzing these images. It should also be noted that the Sentinel-2 sensor system images and InterIMAGE are available free of charge, so it is up to the scientific community to explore them.

Acknowledgements

The Coordination for the Improvement of Higher Education Personnel (CAPES) and the Foundation for Research and Innovation of the State of Santa Catarina (FAPESC).

References

ADDINK, Elisabeth A.; VAN COILLIE, Frieke M.b.; JONG, Steven M. de. Introduction to the GEOBIA 2010 special issue: From pixels to geographic objects in remote sensing image analysis. *International Journal of Applied Earth Observation and Geoinformation*, [s.l.], v. 15, p.1-6, abr. 2012.

BAATZ, Martin; SCHÄPE, Arno. Multiresolution Segmentation: an optimization approach for high quality multi-scale image segmentation. In: *ANGEWANDTE GEOGRAPHISCHE INFORMATIONSVERARBEITUNG*, 12., 2000, Salzburg. Proceedings... Heidelberg: Herbert Wichmann Verlag, 2000. p. 1 - 542.

BHASKARAN, Sunil; PARAMANANDA, Shanka; RAMNARAYAN, Maria. Per-pixel and object-oriented classification methods for mapping urban features using Ikonos satellite data. *Applied Geography*, [s.l.], v. 30, n. 4, p.650-665, dez. 2010.

BRITES, Ricardo Seixas; BIAS, Edilson de Souza; ROSA, Antônio Nuno de Castro Santa. Classificação por Regiões. In: MENESES, Paulo Roberto; ALMEIDA, Tati de. *Introdução ao Processamento de Imagens de Sensoriamento Remoto***.** Brasília: UnB, 2014. Cap. 13. p. 209-220.

CHAOFAN, Wu; JINSONG, Deng; KE, Wang; LIGANG, Ma; TAHMASSEBI, Amir Reza Shah. Object-based classification approach for greenhouse mapping using Landsat-8 imagery. *International Journal of Agriculture and Biological Engineer* 9(1): 79. 2016.

COHENCA, Daniel; CARVALHO, Raquel. Comparação de métodos de classificação OBIA, Máxima Verossimilhança e Distância Mínima em imagem OLI/Landsat-8 em área de alta diversidade de uso do solo. In: *SIMPÓSIO BRASILEIRO DE SENSORIAMENTO REMOTO*, 16. Anais... . João Pessoa: Inpe, 2015. p. 1035 - 1042.

CONGALTON, Russell G. A review of assessing the accuracy of classifications of remotely sensed data. *Remote Sensing of Environment*, [s.l.], v. 37, n. 1, p.35-46, jul. 1991.

CONGALTON, Russell G. A Comparison of Sampling Schemes Used in Generating Error Matrices for Assessing the Accuracy of Maps Generated from Remotely Sensed Data. *Photogrammetric Engineering and Remote Sensing*, [s.l.], v. 54, n. 5, p.593-600, maio 1988.

CONGALTON, Russell G.; GREEN, Kass. *Assessing the accuracy of Remotely Sensed Data:* Principles and Pratices. 2. ed. New York: Crc Press, 2008. 183 p.

COHEN, Jacob. A Coefficient of Agreement for Nominal Scales. *Educational and Psychological Measurement*, [s.l.], v. 20, n. 1, p.37-46, abr. 1960. SAGE Publications.

CRÓSTA, Álvaro Penteado. *Processamento digital de imagens de sensoriamento remoto.* Campinas, SP: IG/UNICAMP, 1992. 170p.

ESA, European Space Agency. *Sentinel-2 User Handbook.* Paris: Esa, 2015. 64 p.

GAO, Jay. Mapping of Land Degradation from ASTER Data: A Comparison of Object-Based and Pixel-Based Methods. *Giscience & Remote Sensing*, [s.l.], v. 45, n. 2, p.149-166, abr. 2008.

HELLDÉN, Ulf. *A Test of Landsat-2 Imagery and Digital Data for Thematic Mapping: Illustrated by an Environmental Study in Northern Kenya*. Lund: University Of Lund, 1980. 63 p.

JEBUR, Mustafa Neamah et al. Per-pixel and object-oriented classification methods for mapping urban land cover extraction using SPOT 5 imagery. *Geocarto International*, [s.l.], v. 29, n. 7, p.792-806, 13 nov. 2013.

LANDIS, J. Richard; KOCH, Gary G.. The Measurement of Observer Agreement for Categorical Data. *Biometrics*, [s.l.], p.159-174, mar. 1977.

MENESES, Paulo Roberto; SANO, Edson Eyji. Classificação Pixel a Pixel de Imagens. In: MENESES, Paulo Roberto; ALMEIDA, Tati de. *INTRODUÇÃO AO PROCESSAMENTO DE IMAGENS DE SENSORIAMENTO REMOTO*. Brasília: UnB, 2014. Cap. 12. p. 191-208.

MORAES, Sofia Royer. *ABORDAGEM GEOBIA PARA A CLASSIFICAÇÃO DO USO E COBERTURA DA TERRA EM ÁREA URBANA ASSOCIADAS AO DESENVOLVIMENTO DE FRAMEWORK PARA MONITORAMENTO DE INUNDAÇÕES NO MUNICÍPIO DE LAJEADO/RS.* 2018. 104 f. Dissertação (Mestrado) - Curso de Programa de Pós-graduação em Sensoriamento Remoto e Geoprocessamento, Universidade Federal do Rio Grande do Sul, Porto Alegre, 2018.

PINHO, Carolina Moutinho Duque de; FEITOSA, Flávia da Fonseca; KUX, Hermann. Classificação automática de cobertura do solo urbano em imagem IKONOS: Comparação entre a abordagem pixel-a-pixel e orientada a objetos. In: *SIMPÓSIO BRASILEIRO DE SENSORIAMENTO REMOTO*, 12., 2005, Goiânia. Anais... São José dos Campos: Inpe, 2005. p. 4217 - 4224.

PRUDENTE, Victor H. R; SILVA, Bruno B. da; JOHANN, Jerry A.; MERCANTE, Erivelto; OLDONI, Lucas V. COMPARATIVE ASSESSMENT BETWEEN PER-PIXEL AND OBJECT-ORIENTED FOR MAPPING LAND COVER AND USE. *Engenharia Agrícola*, [s.l.], v. 37, n. 5, p.1015-1027, set. 2017. FapUNIFESP.

QIU, Bingwen; LU, Difei; TANG, Zhenghong; CHEN, Chongcheng; ZOU, Fengli. Automatic and adaptive paddy rice mapping using Landsat images: Case study in Songnen Plain in Northeast China. *Science of The Total Environment*, [s.l.], v. 598, p.581-592, nov. 2017.

SUAREZ, Alerson Falieri; CANDEIAS, Ana Lúcia Bezerra. AVALIAÇÃO DE ACURÁCIA DA CLASSIFICAÇÃO DE DADOS DE SENSORIAMENTO REMOTO PARA O MUNICÍPIO DE MARAGOGIPE. In: *SIMPÓSIO BRASILEIRO DE CIÊNCIAS GEODÉSICAS E TECNOLOGIAS DA GEOINFORMAÇÃO*, 4., 2012, Recife. Anais... Recife: UFPE, 2012. p. 001 - 0010.

TEHRANY, Mahyat Shafapour; PRADHAN, Biswajeet; JEBUV, Mustafa Neamah. A comparative assessment between object and pixel-based classification approaches for land use/land cover mapping using SPOT 5 imagery. *Geocarto International*, [s.l.], v. 29, n. 4, p.351-369, 5 abr. 2013.